

# Measurement and Correction of Gradient Nonlinearity by Spherical Harmonic Fitting using the ADNI Phantom

Shengzhen Tao<sup>1</sup>, Joshua D. Trzasko<sup>1</sup>, Jeffrey L. Gunter<sup>1</sup>, Seung-Kyun Lee<sup>2</sup>, Ek T. Tan<sup>2</sup>, Yunhong Shu<sup>1</sup>, Kaelly B. Thostenson<sup>1</sup>, and Matt A. Bernstein<sup>1</sup>  
<sup>1</sup>Mayo Clinic, Rochester, MN, United States, <sup>2</sup>GE Global Research, Niskayuna, NY, United States

**Target Audience:** MRI physicists and gradient coil designers.

**Background:** Standard spatial encoding in MRI assumes uniform gradients, but in practice, implementing gradient linearity over the entire imaging field-of-view (FOV) is usually not feasible. Gradient non-linearity, if not properly compensated, causes geometric image distortion<sup>1,2</sup>. Standard strategies to correct gradient non-uniformity on commercial systems (e.g., “GradWarp” or gradient distortion correction)<sup>3,4</sup> are based on a parameterization of the gradient field and typically contain up to 5<sup>th</sup> order terms in the expansion. The correction coefficients are predetermined and the same set of coefficients is applied to all systems in the field. The purpose of this work is to develop a simple method to measure and fit the gradient correction on a per-system basis using the Alzheimer’s Disease Neuroimaging Initiative (ADNI) phantom<sup>5</sup>. A 3D spherical harmonic approximation of the distortion is then determined and used for correction.

**Methods:** The ADNI phantom contains 160 fiducial spheres (with a diameter of 1.0 or 1.5 cm) that are distributed within a 20-cm diameter spherical shell.

The spatial positions of the spheres can be tracked using the AQUAL analysis software that is available with the phantom (see Ref. 6 for details). Differences between the expected locations of the fiducials and their positions measured from the distorted image can be expressed using a spherical harmonic model as in Eq.1, where  $\mathbf{x}$  and  $\mathbf{x}'$  are measured and expected location in Cartesian coordinates, respectively,  $\mathbf{r}$ ,  $\theta$ , and  $\phi$  are polar coordinates,  $P_{mn}$  is the associated Legendre polynomial,  $N$  is the approximation order, and  $\mathbf{A}_{nm}$  and  $\mathbf{B}_{nm}$  are model coefficients. Denoting  $\mathbf{H}$  as the spherical harmonic basis and  $\mathbf{c}$  the corresponding coefficient vector form, the right-hand side of Eq. 1 can be stated as  $\mathbf{H}\mathbf{c}$ , and  $\mathbf{c}$  can be estimated via the constrained optimization process in Eq. 2, where the constraint represents optional *a priori* knowledge of gradient system design. For example, if the gradient system design is symmetric about isocenter, we expect the even order terms to be zero. Such a constraint can be represented by setting  $c_k=0$ , where  $c_k$  is the coefficient of the  $k$ th null term. To test the proposed strategy, an 3D MP-RAGE sequence was performed on 3T GE Signa HDxt system (acquisition plane:sagittal,  $N_x=N_y=256$ ,  $N_z=196$ ,  $\Delta x=1.05\text{mm}$ ,  $\Delta z=1.3\text{mm}$ ) using the whole-body gradient with maximum gradient amplitude and slew rates of 40mT/m and 200mT/m/msec, respectively. The phantom was placed close to the scanner isocenter, and the slight shifting and rotation from the isocenter was estimated and corrected by rigid transformation. The spherical harmonic model was then constructed and the model coefficients were solved by the Nesterov’s optimal gradient method<sup>7,8</sup>, with an iteration number 50. The symmetry of the gradient system was taken into account by constraining the even-order coefficients to be zero. Finally, image distortion was corrected by cubic spline interpolation using the estimated coefficients, and the corrected images were compared against images acquired without Gradwarp.

**Results:** Examples of images before and after (1<sup>st</sup>/2<sup>nd</sup> row) the proposed gradient nonlinear correction with spherical harmonics of order  $N=5$  are shown in Fig 1. Fig. 2 shows the error in fiducial displacement versus displacement along the three magnet axes, before and after correction. The geometrical distortion, which is most apparent in the sagittal and coronal planes, is successfully corrected (Fig. 1). The displacements of the fiducials due to nonlinear gradients can be effectively reduced by the proposed method, as illustrated in Fig. 2. The radial residual mean squared error (RMSE) was reduced from 3.27 mm to 0.32 mm after correction.

**Discussion:** Ref. 6 reported that correction with scanner vendor-provided gradient warping method reduced the RMSE to about 0.3 mm, and we typically use 0.35 mm as cutoff point during quality control tests in the ADNI study. Comparably, the proposed method is able to achieve a similar degree of correction as vendors’ 3D correction. We emphasize however, that neither a vendor correction nor knowledge of the vendor’s correction coefficients are required for the proposed method, suggesting its potential use as an independent characterization and correction for the gradient system. The method is also flexible and can account for non-zero, even-order correction terms that are expected to be present in asymmetric, high-performance gradient coils, which are of interest for a head-only system<sup>9</sup>. The 20-cm diameter of the ADNI phantom is well-matched to a typical head scan FOV. We also expect the method can be readily extended to include higher-order terms (i.e.,  $N>5$ ), if needed.

**Conclusions:** In this work, we have demonstrated that geometrical distortion due to gradient nonlinearity can be successfully measured from image data acquired with the ADNI phantom and corrected via spherical harmonics fitting. The proposed method does not require direct measurement of the magnetic field or detailed knowledge of gradient coil design, and thus can be used in a variety of settings. While feasibility of the method was demonstrated on a symmetric gradient system whose even-order correction coefficients are zero, the method is expected to be flexible enough to handle an asymmetric gradients, such as those used in a head-only system.

**References:** [1] L. Schad et al., MRI 10:609-21, 1992; [2] S. Doran et al., Phys Med Biol 50:1343-61, 2005; [3] G. Glover et al., U.S. Patent 4591789, 1986; [4] A. Janke et al., MRM 52(1):115-22, 2004; [5] C. Jack, Jr., et al., JMIR 27(4):685-91, 2008; [6] J. Gunter et al., Med Phys 36(6):2193-2205, 2009; [7] Y. Nesterov et al., Sov Math Dokl 27:372-6, 1983; [8] B. O’Donoghue et al., Found Comput Math. In press. [9] J. Mathieu et al., ISMRM 2013: 2708.

**Acknowledgements:** This work was supported in part by the NIH grant 5R01EB010065.

$$\mathbf{x}' - \mathbf{x} \approx \sum_{n=0}^N \sum_{m=0}^n \mathbf{r}^n P_{mn}(\cos \theta) (\mathbf{A}_{nm} \cos m\phi + \mathbf{B}_{nm} \sin m\phi) - \text{Eq. 1}$$

$$\mathbf{c} = \arg \min \|\mathbf{H} \cdot \mathbf{c} - (\mathbf{x}' - \mathbf{x})\|_2^2, \quad \text{s. t. } \mathbf{c} \in \mathcal{C}. - \text{Eq. 2}$$

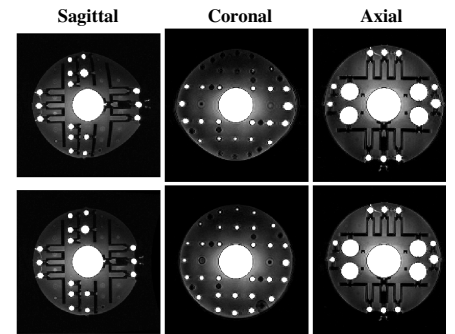


Fig 1. Examples of images before (1<sup>st</sup> row) and after (2<sup>nd</sup> row) correction with spherical harmonics of order  $N=5$

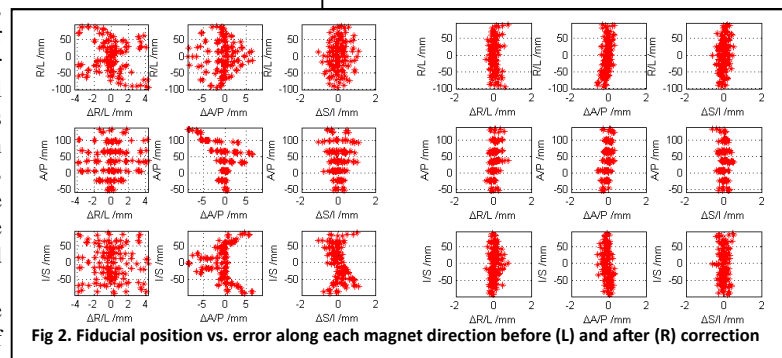


Fig 2. Fiducial position vs. error along each magnet direction before (L) and after (R) correction